# Characterization of Radiation Exposure at Aviation Flight Altitudes Using the Nowcast of Aerospace Ionizing Radiation System (NAIRAS)

**Daniel B. Phoenix[1,2,3], Chris J. Mertens[3], Guillaume P. Gronoff[2,3], and Kent Tobiska[4]**

[1.] Analytical Mechanics Associates, Hampton, VA, USA
[2.] Science Systems and Applications, Inc., Hampton, VA, USA
[3.] NASA Langley Research Center, Hampton, VA, USA
[4.] Space Environment Technologies, Pacific Palisades, CA, USA

Corresponding author: Daniel B. Phoenix (daniel.b.phoenix@nasa.gov)

**Key Points**

- The ARMAS dosimeter flew on board and measured dose rates for 39 corporate and 6 research flights between August 2022 and March 2023.
- The NAIRAS Run on Request model was run for each flight and produces dose estimates in agreement with the ARMAS dosimeter.
- Results show that airline crew radiation exposure does not exceed the ICRP standard but could invoke individual radiation monitoring.

## Abstract

Exposure to ionizing radiation from galactic cosmic rays (GCR) and solar energetic particles (SEP) at aircraft flight altitudes can have an adverse effect on human health. Although airline crews are classified as radiation workers by the *International Commission on Radiological Protection (ICRP)*, in most countries, their level of exposure is unquantified and undocumented throughout the duration of their career. As such, there is a need to assess pilot ionizing radiation exposure. The Nowcast of Aerospace Ionizing RAdiation System (NAIRAS), a real-time, global, physics-based model is used to assess such exposure. The Automated Radiation Measurements for Aerospace Safety (ARMAS) measurement dataset consists of high latitude, high altitude, and long-duration aircraft flights between 2013-2023. Here, we characterize radiation exposure at aviation flight altitudes using the NAIRAS model and compare with 45 flight trajectories from the recent ARMAS flight measurement inventory.



## Plain Language Summary

The Nowcast of Aerospace Ionizing RAdiation System (NAIRAS) model and the Automated Radiation Measurements for Aerospace Safety (ARMAS) dosimeter were used to estimate radiation exposure for airline crews. Radiation dose rates were measured and calculated for 45 fairly representative flights between August 2022 and March 2023. Model results showed good agreement with the dosimeter and suggest that although airline crews on these flights were not exposed to radiation at levels exceeding the international standard, they would be candidates for individual radiation monitoring.


## 1 Introduction

Aircraft flying at typical commercial and corporate airline altitudes in the upper troposphere and lower stratosphere are constantly exposed to extraterrestrial, high-energy charged particles and secondary neutrons. Energetic particles at these altitudes can affect aircraft microelectronic systems and the health of airline crews and passengers (Wilson, 2000; IEC, 2006). This type of particle radiation comes from two main sources: (1) the ever-present galactic cosmic radiation (GCR), which originates from outside our solar system, and (2) solar energetic particles (SEP), which are associated with eruptions on the Sun's surface and typically only last for several hours to days (Wilson et al., 1991; Gopalswamy et al., 2003).

Due to this exposure, airline crews are classified as radiation workers by the *International Commission on Radiological Protection (ICRP)* (1991). In several recent studies, it was found that airline crews in the United States have received the highest average effective dose among all radiation workers surveyed (NCRP, 2009). Additionally, a study of Air Canada pilots showed that most pilots were exposed to over 1 mSv, with the majority receiving between 3 and 5 mSv (Bennett et al., 2013). An exposure of 1 mSv is enough to warrant an individual exposure assessment in some countries (Linborg and Nikjoo, 2011). Furthermore, the flights on high-latitude or intercontinental routes are at risk of exceeding the maximum public and prenatal exposure during a single SEP event or through several (~5-10) round-trip, high-latitude flights from GCR exposure (AMS, 2007; Copeland et al., 2008; Dyer et al., 2009; Mertens et al., 2012). Importantly, while some countries do monitor airline crew exposure, many countries do not, making airline crews the only occupational group to be exposed to both unquantified and undocumented levels of radiation over their career. As such, there is a need to develop tools to

extend the current scientific knowledge of the atmospheric ionizing radiation field for the benefit of decision making and planning within the aviation community.

Currently, there are a number of models for assessing radiation exposure available to the aviation community. The following models have been recently compared: the CARI-7A (Civil Aeromedical Research Institute) model (Copeland et al., 2010; Copeland, 2017), which is used by the Federal Aviation Administration, the PANDOCA (Professional Aviation Dose Calculator) model (Matthiä et al., 2013, 2014), which is used by the German Aerospace Center, and the Nowcast of Aerospace Ionizing RAdiation System (NAIRAS, Mertens et al., 2023b). Previous efforts to evaluate model calculated radiation doses at aviation cruise altitudes have been limited by the availability of reliable high-quality dose rate measurements, particularly for the severe, high dose radiation events. Nevertheless, model evaluation studies have been performed using measurements of the omnipresent background radiation environment from galactic cosmic radiation (GCR). In Meier et al. (2018), the CARI-7A, PANDOCA, and NAIRAS models were evaluated using observations from two flight missions: the Comparison of Airborne RAdiation Measuring Equipment for implementation of Legal requirements (CARAMEL) campaign (Wissmann et al., 2010) and the COmparison of COsmic Radiation Detectors (CONCORD) campaign (Meier et al., 2016). The intercomparison showed that all three models were within 20% of the measurements.

Recent improvements in NAIRAS necessitate an updated evaluation of the model's performance. Additionally, a NASA award was granted to have the ARMAS dosimeter fly on Raytheon corporate flights from August 2022 to April 2023. This new dataset provides an excellent opportunity to (1) evaluate dose rates representative of typical commercial/corporate aircraft routes, (2) evaluate new NAIRAS dose rate calculations for the flight trajectories and compare with ARMAS dosimeter measurements, and (3) compare the dose rate calculations from the previous version of NAIRAS (version 2.0) and the latest version of the model (version 3.0).

## 2 NAIRAS Model Description

The NAIRAS model is a real-time, global, physics-based model developed to calculate radiation exposure to airline crews from both galactic cosmic radiation and solar radiation. The NAIRAS model has been documented previously (Mertens et al., 2010, 2012, 2013). The latest version is described in Mertens et al. (2023a, 2023b, 2023c) and includes several updates, particularly the expansion of the GCR composition, multi-directional atmospheric transport, an improved SEP spectral fitting algorithm, and the inclusion of terrestrial trapped protons (TRP). Here, we summarize the key features of the latest version of the model.

The GCR composition in the H-BON10 model was expanded to calculate LET spectra out to 100 MeV-cm$^2$/mg. Previously, the highest charge and heaviest nuclear isotope in the version of the H-BON10 model was nickel (Z = 28, A = 58). The new version of NAIRAS has extended the composition of the H-BON10 model to include ultra-heavy GCR nuclear isotopes, with the highest charge and heaviest isotope being uranium (Z = 92, A = 238).

To account for the expanded GCR composition, 116 coupled transport equations along each ray direction are required. In the previous version of NAIRAS, the GCR and SEP differential flux at the top of the boundary of the neutral atmosphere was approximated by a projection of a

directionally isotropic source along the vertical direction. Recent measurements during the NASA Radiation Dosimetry Experiment (RAD-X) showed that transport along a single direction is insufficient at predicting dosimetric quantities at high-altitudes above commercial aviation cruise altitudes (Norman et al., 2016). Thus, the atmospheric transport in NAIRAS version 3.0 was updated to include multi-directional transport through the atmosphere. In addition to GCR and SEP sources of radiation, the new version of NAIRAS now also includes terrestrial trapped protons (TRP). The GEOFFB trapped proton belt model was integrated into NAIRAS version 3.0 to extend the model domain from the atmospheric ionizing radiation environment to the geospace radiation environment (Badavi et al., 2011).

A new proton spectral fitting code was developed in NAIRAS version 3.0 that allows the option to fit a SEP proton spectrum to either the differential GOES proton flux channels or the integral proton flux channels. SEP spectral fitting to the GOES differential proton flux channels has been proven to be problematic during the onset of SEP events and during weak-to-moderate events. The new option to infer the SEP spectrum using GOES integral proton flux channels has enabled a spectrum to be obtained that is consistent with the GOES differential proton channels using a method that is robust against numerical instability and free from erroneous, non-physical fits (see Mertens et al., 2023a, Figure 4).

Transmission of GCR and SEP ions through the geomagnetic field has been improved to capture additional complexities by scaling the numerically-determined vertical cutoff rigidity to other arrival directions. The cutoff rigidity model now also includes an option to use the T89 magnetospheric field model (Tsyganenko, 1989), which only needs the Kp-index as an input quantity to calculate the dynamical response to solar-geomagnetic variability. Although the T89 model does not capture the magnetospheric response to geomagnetic variability as well as the TS05 model (Tsyganenko and Sitnov, 2005), it does allow for historical solar-geomagnetic storm events to be analyzed prior to 1995.

## 3 ARMAS Flight System

The ARMAS Flight Module (ARMAS FM) unit consists of two components: a flight instrument that measures the real-time radiation total ionizing dose (TID) environment on the aircraft and a calibrated data stream from the aircraft to the ground (Tobiska et al., 2016) using the ARMAS v10.41 and v10.42 data processing systems. The ARMAS system uses a Teledyne micro dosimeter (uDOS001), which directly measures TID absorbed by an internal silicon test mass. The micro dosimeter measures energy absorbed from heavy ions, alphas, protons, neutrons, electrons, and gamma rays, providing an accurate measurement of absorbed dose in silicon. As such, the fundamental quantity measured by the ARMAS dosimeter is the absorbed dose in silicon. All other ARMAS dose quantities are derived by empirical scale factors (Tobiska et al., 2016).

The dosimeter operates in a wide range of input power voltages that are >13V DC. The accumulated dose resolution is 0.14 μGy and is capable of making measurements in excess of 1 kGy. The instrument is typically operated in an aircraft cabin (temperature range 15° C to 25° C), which is well within its acceptable operating range (-30° C to +40° C).

## 4 Description of the Flights

Between August 2022 and April 2023, the ARMAS FM 07008 unit was flown on 45 flights, 39 on Raytheon corporate flights and 6 on NASA Langley Research Center (LaRC) airborne science research flights. The majority of these flights occurred in the Northern Hemisphere middle latitudes (30° – 50° N), particularly in the United States (Figure 1). About 30% of the flights were in Europe or transatlantic between Europe and the United States. Only one flight occurred at low latitudes (< 30° N) and crossed the equator.

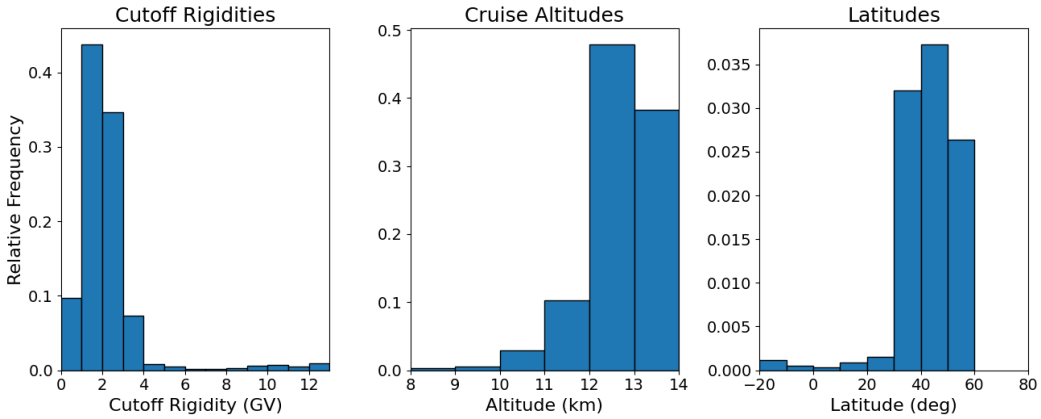


**Figure 1.** Summary of the cutoff rigidities, cruise altitudes, and latitudes of the Raytheon flights.

Additionally, the ARMAS dosimeter collected data on six flights in March 2023 on NASA LaRC research aircraft (Figure 2) during a science mission in Norway. These six flights all occurred at high latitude (generally above 60°N) and low cutoff rigidity (generally less than 1 GV) and typically had a cruise altitude of 11-13 km.

Overall, considering all 45 flights, the cutoff rigidities at cruise altitude ranged from 1-3 GV while the cross-equator flight had a mean cutoff rigidity of 10 GV (Fig. 1). The mean cutoff rigidity of all 45 flights was 2.26 GV. The cruise altitude ranged from 11 – 14 km, with a mean cruise altitude of 12.5 km for all flights.

Flight trajectory information used to run NAIRAS in Run on Request mode was obtained and processed using FlightAware, with aircraft altitudes provided in barometric altitude coordinates. This coordinate system is required for running NAIRAS. The use of GPS altitude coordinates can result in dose rate errors of 50%.

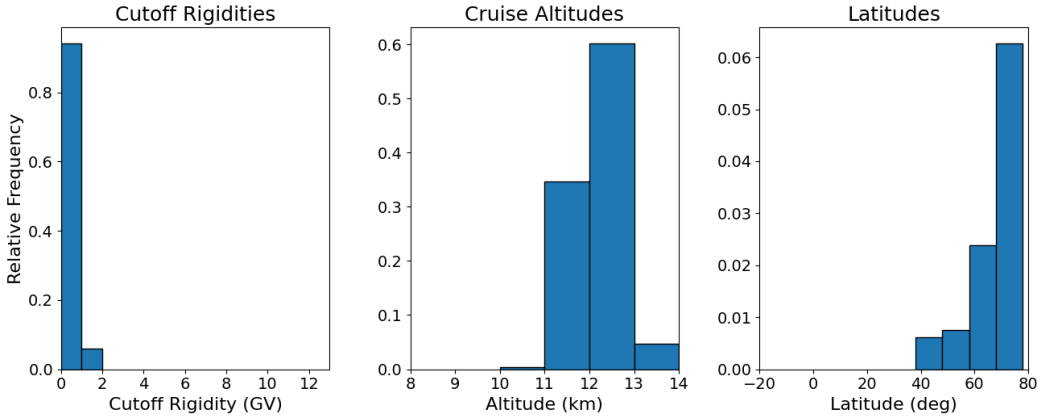


**Figure 2.** As in Figure 1, but for the six NASA LaRC research flights in Norway.

## 5 Results

### 5.1 Summary of ARMAS Dose Rates

The collection of Raytheon flights presented in this study are representative of the airline routes that a corporate airline crew would fly. Using the ARMAS dosimeter measurements, we can obtain an accurate estimate of the typical dose rates these airline crews are exposed to. Due to the characteristics of the ARMAS unit, we consider a few constraints on our dataset. First, we only consider measurements that occurred above 8 km in altitude, as it has been demonstrated that the radiation dose is too low below 8 km to achieve good noise statistics in the ARMAS measurements (Tobiska et al., 2016). For a similar reason, we only consider data taken at aircraft cruising altitude because aircraft ascending or descending too quickly will result in a degraded spatial resolution of the measured data. Since the uncertainty in the ARMAS dosimeter has been demonstrated to be 24% (Tobiska et al., 2016), we discard any cruise altitude segments with an average uncertainty in the ARMAS measured absorbed dose rate in silicon of 24% or greater. We also consider other sources of uncertainty such as the analog to digital conversion and the random variation from GCRs. Lastly, to assess how dose rates vary with cutoff rigidity and latitude, we take the average dose rate over cruise durations of at least 30 minutes but no more than 2 hours.

Using these criteria, ARMAS dose rates for a typical corporate airline crew are calculated and summarized for all cutoff rigidities in Table 1. The median absorbed dose rate in silicon and tissue were 2.8 and 4.2 μGy/h, respectively, the median dose equivalent rate was 8.6 μSv/h, the median ambient dose equivalent rate was 13.3 μSv/h, and the median effective dose rate was 17.8 μSv/h. Therefore, for a typical commercial airline crew flying 800-1000 hours per year, we estimate an annual exposure of 14.2 – 17.8 mSv of effective dose. For a corporate airline crew flying 100 – 400 hours per year and an average of 250 hours per year we estimate an annual exposure of 1.8 – 7.1 mSv (average of 4.5 mSv). Based on the current ICRP recommendations for radiation exposure for a nonpregnant radiation worker, the recommended exposure for a 5-year average is 20 mSv/yr. From this set of Raytheon flights, the airline crew would not be expected to exceed the ICRP recommendation for radiation exposure. However, as noted in Linborg and Nikjoo (2011), an annual exposure of 1 mSv is enough to invoke individual radiation monitoring, particularly in countries that have more stringent radiation standards.

**Table 1.** Mean and median ARMAS dose rates among all cruise altitude segments.

| ARMAS Doses | Si Dose (µGy/h) | Ti Dose (µGy/h) | Dose Eq. (µSv/h) | Ambient Dose (µSv/h) | Effective Dose (µSv/h) |
|---|---|---|---|---|---|
| Mean | 2.8 | 4.1 | 8.5 | 13.1 | 17.7 |
| Median | 2.8 | 4.2 | 8.6 | 13.3 | 17.8 |

5.2 Comparisons of NAIRAS and ARMAS Dose Rates

The NAIRAS Run on Request (RoR) mode was run for each Raytheon flight in the database. The NAIRAS model makes calculations of absorbed dose in silicon, absorbed dose in tissue, ambient dose equivalent, dose equivalent, and effective dose. Assessing the model accuracy of these dose rate calculations enables the utilization of NAIRAS for future aircraft flights and for past flights where dosimeter measurements are not available. This will allow airline crews to estimate radiation exposure over their careers as well as projected exposure on future flights.

As stated above, the ARMAS dosimeter directly measures absorbed dose in silicon. While all four NAIRAS calculated dose rates will be considered, we will focus on the evaluation of the NAIRAS calculated absorbed dose in silicon since it is the fundamental quantity measured by the ARMAS dosimeter. The correlation plot of absorbed dose rate in silicon shows very good agreement between the model and observations (Figure 3a).

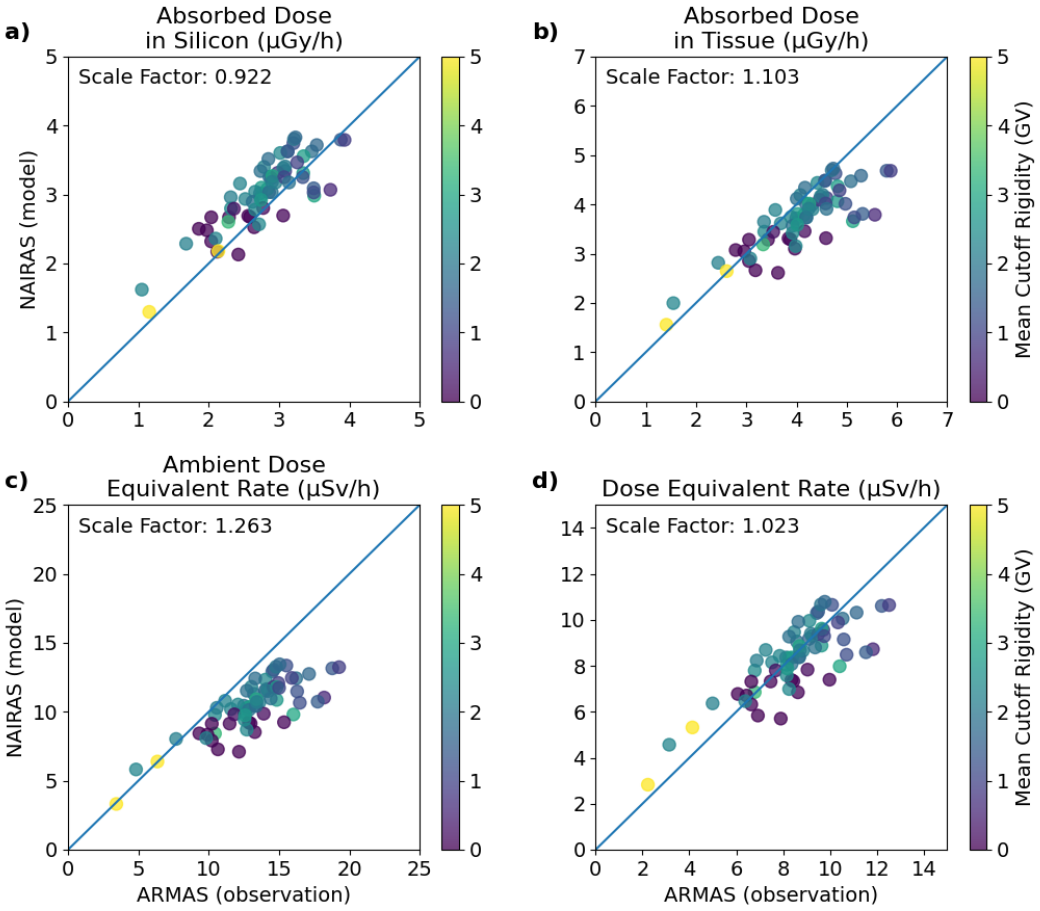


**Figure 3.** Correlation plot of median (a) absorbed dose rate in silicon, (b) ambient dose equivalent rate, (c) dose equivalent rate, and (d) effective dose rate for all ARMAS and NAIRAS cruise altitude segments.

Quantitatively, NAIRAS shows good agreement with the ARMAS dosimeter for absorbed dose in silicon, with a scale factor of 0.922. The percent difference in mean absorbed dose rate in silicon for all the cruise altitude segments reveals a difference of less than 24% for most of the flights (e.g., 59 out of 66 cruise altitude segments) which is notable because the ARMAS margin of error is ~24% (e.g., Tobiska et al., 2016).

Correlation plots of the other three measured and modeled calculated doses reveal similar agreement (Figure 3b-d), with absorbed dose in tissue and dose equivalent rate also showing good agreement (e.g., scale factors of 1.103 and 1.023, respectively). The ambient dose equivalent rate shows a slight underprediction by NAIRAS while the effective dose rate comparison shows a greater underprediction by NAIRAS (scale factor of 1.494) because the ARMAS effective dose rate is derived based on model calculations from NAIRAS version 2.0 (not shown). As with the mean absorbed dose rate in silicon, we also find the percent difference in mean (and median) dose rates to be generally less than 24% for the dose equivalent and

ambient dose equivalent rates. A summary of the median and mean dose rates for ARMAS and NAIRAS and the percent differences are shown in Table 2. Considering all flight segments, the model calculated absorbed dose in silicon, tissue and the dose equivalent rate are in very good agreement with observations (less than 10% difference), while modeled ambient dose equivalent is within 21% of observations.

**Table 2.** Mean and median dose rates for NAIRAS and ARMAS from all cruise altitude segments.

| **Mean Dose** | **Si Dose (µGy/h)** | **Ti Dose (µGy/h)** | **Dose Eq. (µSv/h)** | **Ambient Dose (µSv/h)** | **Effective Dose (µSv/h)** |
|---|---|---|---|---|---|
| ARMAS | 2.8 | 4.1 | 8.5 | 13.1 | 17.7 |
| NAIRAS | 3.0 | 3.7 | 8.3 | 10.4 | 11.9 |
| Difference (%) | 8.27 | -9.29 | -2.35 | -20.97 | -33.05 |
| | | | | | |
| **Median Dose** | **Si Dose (µGy/h)** | **Ti Dose (µGy/h)** | **Dose Eq. (µSv/h)** | **Ambient Dose (µSv/h)** | **Effective Dose (µSv/h)** |
| ARMAS | 2.8 | 4.2 | 8.6 | 13.3 | 17.8 |
| NAIRAS | 3.1 | 3.8 | 8.0 | 10.5 | 11.9 |
| Difference (%) | 7.39 | -9.62 | -6.94 | -21.14 | -32.85 |

To gain a better understanding of the distribution of dose rates measured by ARMAS and calculated by NAIRAS, boxplots of the dose rates for all cruise altitude segments are examined (Figure 4). For all flights, the interquartile range (IQR) for the absorbed dose rate in silicon is 2.5 – 3.1 µGy/h in ARMAS and 2.7 – 3.3 µGy/h in NAIRAS. The absorbed dose rate in tissue IQR is 3.6 – 4.6 µGy/h in ARMAS and 3.3 – 4.1 µGy/h in NAIRAS. The ambient dose equivalent IQR is 11.9 – 14.8 µSv/h in ARMAS and 9.2 – 11.7 µSv/h in NAIRAS. The dose equivalent IQR is 7.7 – 9.6 µSv/h in ARMAS and 7.4 – 9.4 µSv/h in NAIRAS. And the effective dose rate IQR is 15.3 – 20.2 µSv/h in ARMAS and 10.5 – 13.4 µSv/h in NAIRAS. For the absorbed doses (e.g., silicon, tissue) and dose equivalent, there is good overlap between the modeled and observed IQR for the dose rates, particularly the absorbed dose rate in silicon. For ambient dose equivalent rate and effective dose, NAIRAS underestimates the dose rates, however, these are empirically derived dose quantities from ARMAS.

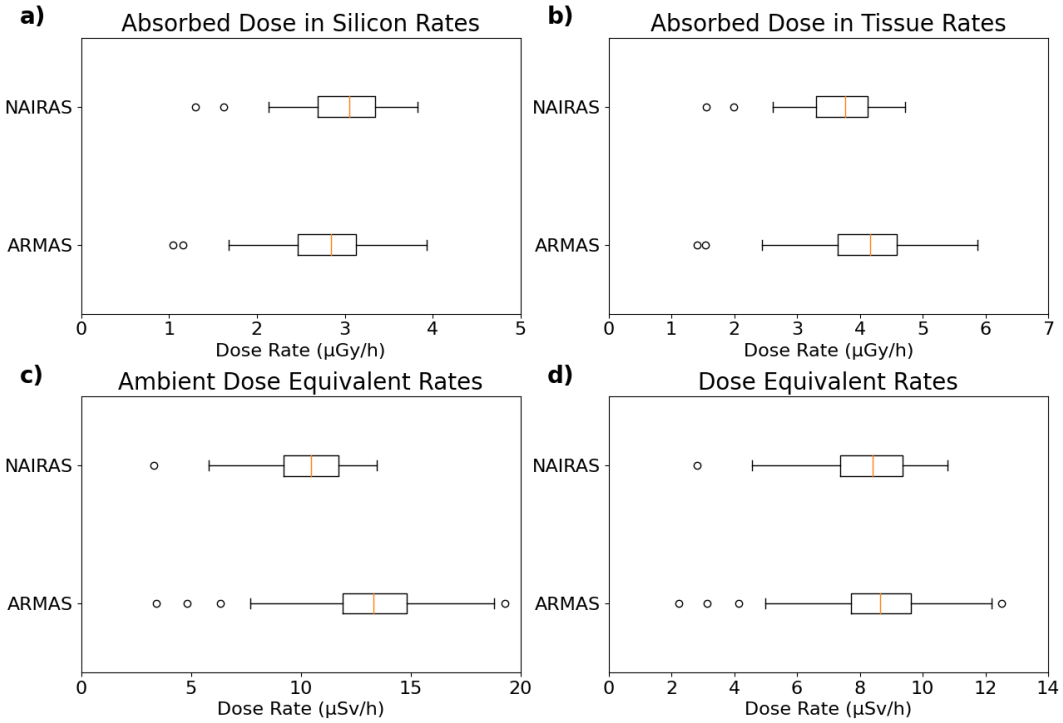


**Figure 4.** Distributions of ARMAS measured and NAIRAS calculated dose rates for all flights and cutoff rigidities.

Lastly, we summarize absorbed dose in silicon by cutoff rigidity. The majority of flights occurred in regions of low cutoff rigidity (0 – 4 GV). For flights in this radiation environment, the absorbed dose in silicon ranges from ~2.5 - 3.5 µGy/h. Interestingly, the median dose rate is highest for flights in the 1 -2 GV range. However, this is likely due to the higher cruise altitudes at these lower latitude flights (compared to flights in the 0 – 1 GV range). For high cutoff rigidity environments (8 – 12 GV), the median dose rate is generally between 1.2 – 1.7 µGy/h, well over 1 µGy/h lower than flights in the 0 – 4 GV range (Table 3).

**Table 3.** Median Si Dose Rate by Cutoff Rigidity (µGy/h)

| Cutoff Rigidity Range | NAIRAS | ARMAS | Number of Qualifying Trajectory Points |
|---|---|---|---|
| 0 – 1 GV | 2.7 | 2.5 | 2206 |
| 1 – 2 GV | 3.5 | 3.4 | 2486 |
| 2 – 3 GV | 3.1 | 2.5 | 1840 |
| 3 – 4 GV | 2.9 | 2.5 | 333 |
| 4 – 5 GV | 2.7 | 2.5 | 44 |
| 5 – 6 GV | 2.4 | 2.5 | 33 |
| 6 – 7 GV | 2.2 | 1.7 | 9 |
| 7 – 8 GV | 1.9 | 2.5 | 9 |
| 8 – 9 GV | 1.7 | 1.7 | 17 |

| | | | |
|---|---|---|---|
| 9 – 10 GV | 1.5 | 1.7 | 33 |
| 10 – 11 GV | 1.4 | 1.7 | 44 |
| 11 – 12 GV | 1.3 | 0.8 | 30 |

## 5.3 Case Study 1: Domestic Flight from San Jose, CA to Hartford, CT

To illustrate the dose rates over a typical cross-country domestic flight, timeseries plots of the four dose rates are shown for a flight from Tucson, AZ to Hartford, CT (Figure 5). This flight is characterized by a mean cruise altitude of 12.5 km and mean latitude of 37.88° N.

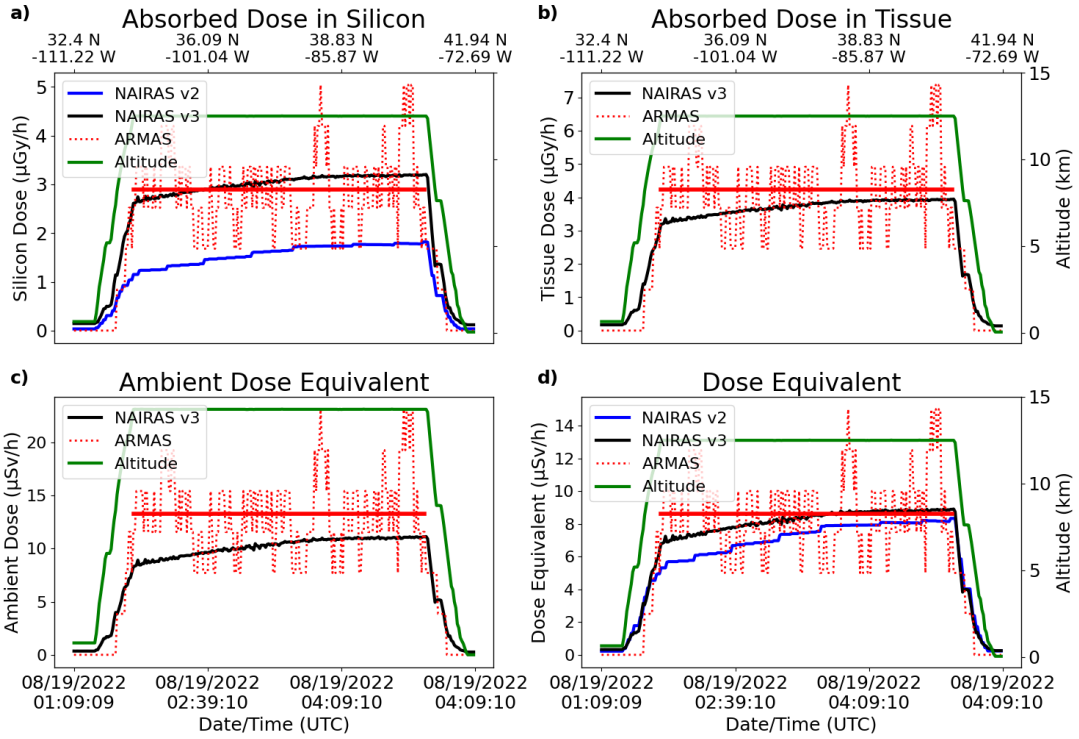


**Figure 5.** Timeseries plots of (a) absorbed dose rate in silicon, (b) absorbed dose rate in tissue, (c) ambient dose equivalent, and (d) dose equivalent for the August 19, 2022 01:09 UTC flight from Tucson, AZ to Hartford, CT. The green line shows aircraft altitude (right axis), the red line shows the ARMAS dose rate (left axis), the red dashed line shows the mean ARMAS dose rate at cruise altitude (left axis), and the black line shows the NAIRAS dose rate (left axis).

The cutoff rigidity for this flight ranges from 1.4 GV to 3.5 GV (Figure 6a). Overall, there is very good agreement between NAIRAS and the ARMAS dosimeter. At cruise altitude, the mean absorbed dose in silicon is 2.9 and 3.0 µGy/h in ARMAS and NAIRAS, respectively, a 4.14% difference. As in Figure 6a, the cutoff rigidity is 4.1 GV at the beginning of the flight and decreases to ~1.7 GV. The NAIRAS and the ARMAS dose rates show a slight increase in the dose rate over the duration of the flight, reflecting this change in cutoff rigidity, while the cruise altitude remains constant. Compared to NAIRAS version 2.0, the latest updates to NAIRAS produce higher dose rates for all modeled dose quantities and are in much better agreement with the dosimeter.

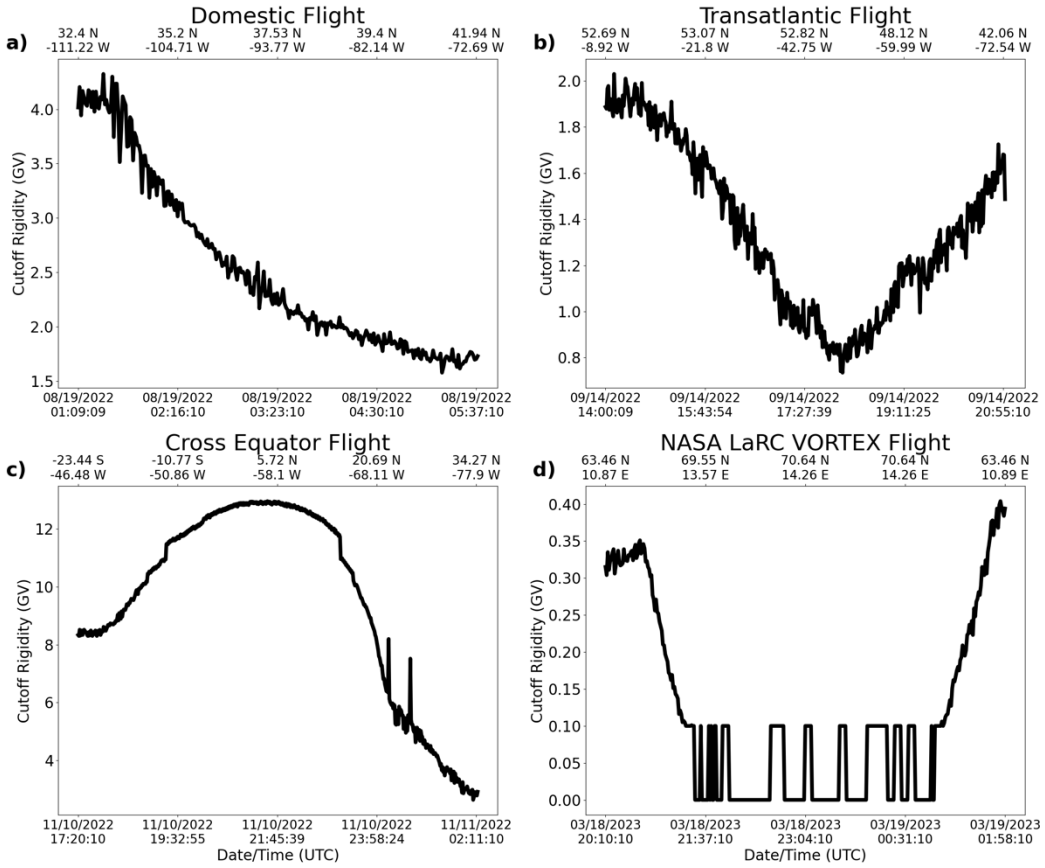


**Figure 6.** Timeseries of cutoff rigidity (GV) for (a) a typical United States domestic flight from Tucson, AZ to Hartford, CT, (b) a transatlantic flight from Shannon, Ireland to Hartford, CT, USA, (c) a cross-equator flight from São Paulo, Brazil to Wilmington, NC, USA, and (d) a high latitude flight in Norway.

5.4 Case Study 2: Transatlantic Flight from Shannon, Ireland to Hartford, CT, USA

To illustrate typical dose rates for an international flight, particularly one that approaches a cutoff rigidity of 0 GV (Fig. 6b), timeseries of dose rates and cutoff rigidity are shown from a flight from Shannon, Ireland to Hartford, CT, USA. This flight had cruise altitude segments of 12.19 km (mean latitude of 52.49° N) and 12.89 km (mean latitude of 46.75° N). For the two cruise altitude segments, the mean ARMAS measured absorbed dose rate in silicon is 3.0 and 3.2 µGy/h and the mean NAIRAS calculated absorbed dose rate in silicon is 3.3 and 3.7 µGy/h (Fig. 7). For the two cruise altitude segments, the percent difference in mean absorbed dose rate in silicon is 10.04% and 16.84%, both within the margin of error of the ARMAS dosimeter. Interestingly, the highest dose rate does not occur during the minima in cutoff rigidity, but rather the highest cruise altitude, demonstrating that GCR dose rate has a higher dependence on altitude than cutoff rigidity. This result is consistent with Tobiska et al. (2016) who showed that the dose rate doubles for every 2 km increase in altitude. As in the domestic flight, the NAIRAS version

3.0 dose rates are all higher than in version 2.0 and are generally in better agreement with ARMAS.

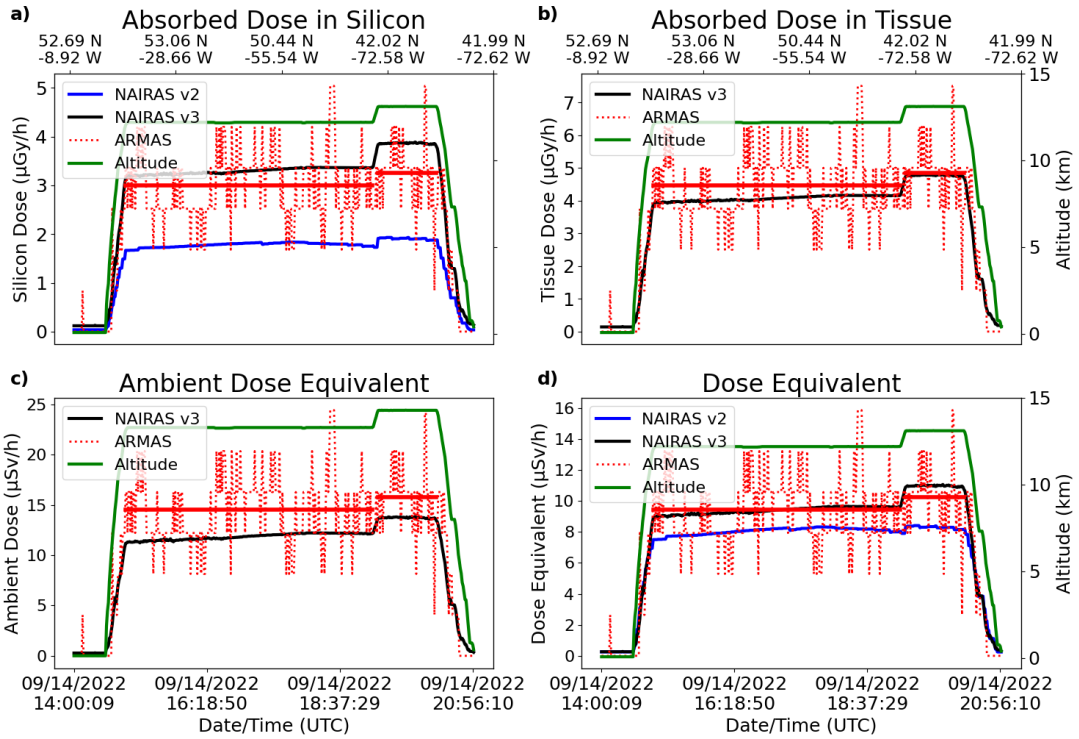


**Figure 7.** As in Figure 5, but for the transatlantic flight from Shannon, Ireland to Hartford, CT, USA.

5.5 Case Study 3: Cross-Equator Flight from São Paulo, Brazil to Wilmington, NC, USA

One flight in this dataset crossed the equator. As such, it represents a demonstration of dose rates at low latitudes and high cutoff rigidities. The flight departed from São Paulo, Brazil at a relatively low latitude (23.44°S) and high cutoff rigidity (~8 GV) before crossing the equator and reaching the highest cutoff rigidity for any flight in this dataset (~13 GV). As the flight continues to the north towards the northern hemisphere mid-latitudes, the cutoff rigidity rapidly decreases (Fig. 6c), and dose rates increase (beginning 11/10/2022 ~23:00 UT).

For the two cruise altitude segments (12.23 km, 13.11 km), the mean absorbed dose in silicon is 1.2 and 2.1 µGy/h in ARMAS, respectively, and 1.3 and 2.2 µGy/h in NAIRAS, respectively (Fig. 8). The percent differences for these two cruise altitude segments are 12.43% and 1.98%, both well within the ARMAS margin of error. Compared to the international and domestic flights, which were both in the northern hemisphere mid-latitudes, the average dose rate for this flight is about 50% lower. Similar to the previous two flights, NAIRAS version 3.0 shows much better agreement than NAIRAS version 2.0 (NAIRAS version 2.0 absorbed dose in silicon was 70% lower than ARMAS, NAIRAS version 3.0 only 5% lower than ARMAS).

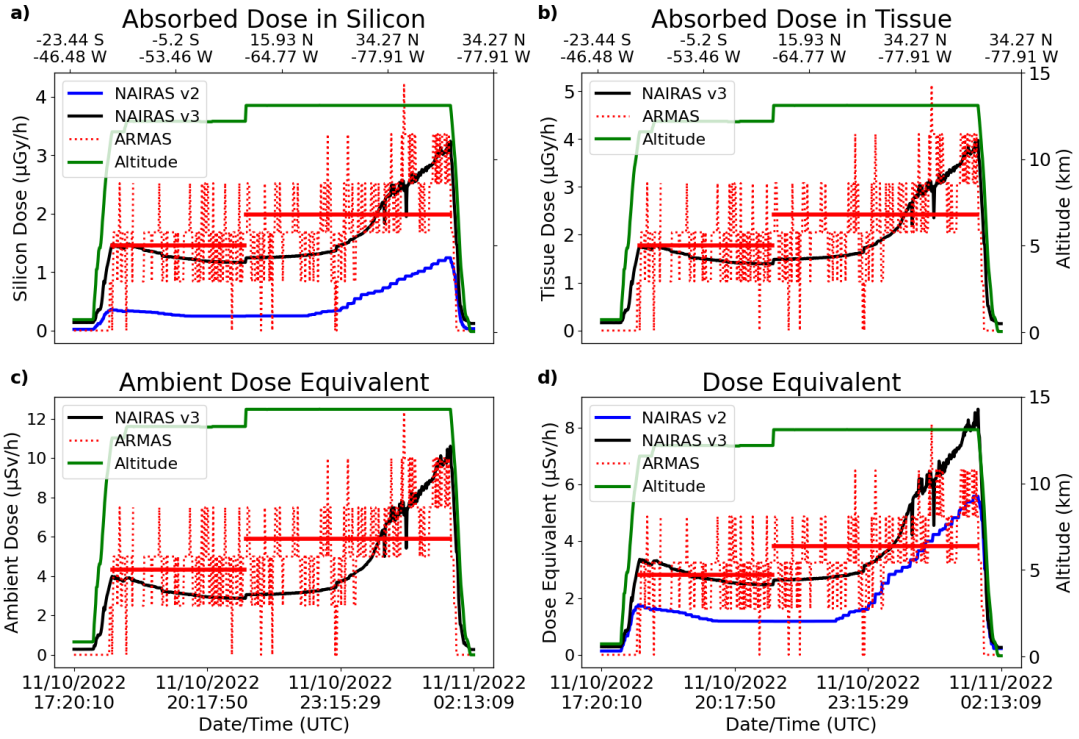


**Figure 8.** As in Figure 5, but for a cross-equatorial flight from São Paulo, Brazil to Wilmington, NC, USA.

5.6 Case Study: NASA Langley Research Flight in Norway

Several high-latitude flights took place in March 2023 with the ARMAS dosimeter as part of a NASA LaRC Vorticity Experiment (VortEx) Norway Sounding Rocket Mission. In contrast to the Raytheon corporate flights, these were research flights designed to study large vortices in the upper atmosphere. These flights provide an interesting contribution to the dataset due to the low cutoff rigidity (near 0 GV for the duration of the flight (Fig. 6d)), which represents a typical high-end for radiation dose exposure. For these flights, the NAIRAS-calculated dose rates agree quite well with the ARMAS measurements (Figure 9). For the flight shown in Figure 9, the mean dose rate in silicon is 2.5 µGy/h and 2.7 µGy/h from ARMAS and NAIRAS, respectively, with a mean percent difference of 8.9%. The mean latitude for this flight is 69.8°N and the mean cutoff rigidity is 0.05 GV (Fig. 6d). Unlike the other flights discussed above, there is little difference between the NAIRAS version 2.0 and version 3.0 dose rates, with the exception of the absorbed dose rate in silicon. Overall, NAIRAS version 3.0 is an improvement over NAIRAS version 2.0.

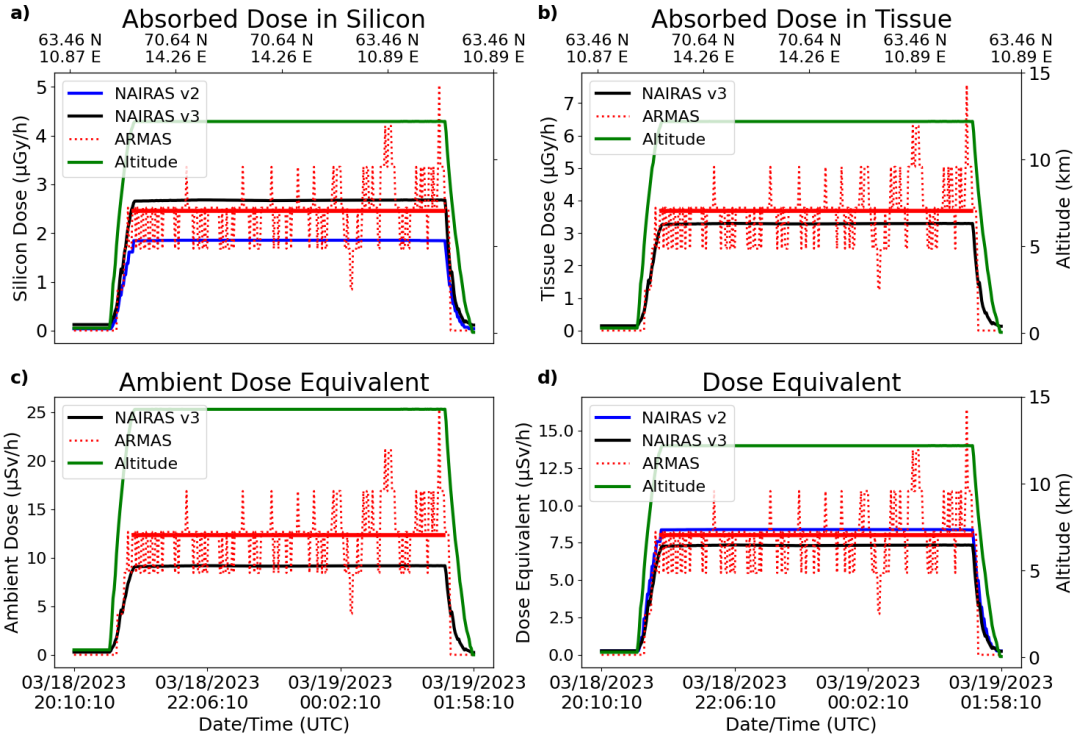


**Figure 9.** As in Figure 5, but for a NASA LaRC research flight in Norway (Trondheim Airport, Værnes).

5.7 Improvements over NAIRAS version 2.0

The main improvements in NAIRAS version 3.0 are the extension of the atmosphere to free-space and inclusion of multi-directional ray transport, improvements to the SEP proton spectral fitting algorithm, and the inclusion of GCR ultra-heavy ions. The multi-directional transport improves the absorbed dose quantities (e.g., absorbed dose in silicon, tissue) which are sensitive to the charged particle environment. Additionally, the expansion of the GCR ultra-heavy ions from nickel (Z = 28, A = 58) to uranium (Z = 92, A = 238) increases the maximum LET from 31.9 MeV-cm$^2$/mg to 110.2 MeV-cm$^2$/mg (Mertens et al., 2023a). This update to NAIRAS version 3.0 also increases the dose rates at aircraft cruise altitudes. Together these updates have yielded an increase especially in absorbed dose rate calculations, bringing the model in much better agreement with the dosimeter measurements. For calculations of absorbed dose in silicon among the four flights discussed in detail in Sections 5c-f, NAIRAS version 3.0 dose rates are both higher than NAIRAS version 2.0 and in better agreement with the ARMAS dosimeter. In general, differences in absorbed dose rates between NAIRAS version 2.0 and ARMAS are 30% greater for the cruise altitude segments in this study, compared to NAIRAS version 3.0 and ARMAS percent differences.

## 6 Summary and Future Work

Dose rate measurements from the ARMAS FM dosimeter on board 39 Raytheon corporate and 6 NASA LaRC research flights provide a good range in expected dose rates for airline crews. Considering all flights, the ARMAS derived median effective dose rate of 17.8 µSv/h, which yields an annual dose exposure of 17.8 mSv for a flight crew flying 1000 hours per year. For a corporate airline crew flying 400 hours per year, it is estimated that the crew would be exposed

to a total of 7.1 mSv. However, based on comparisons with the NAIRAS model, it is likely that the ARMAS derived effective dose rate should be reevaluated with NAIRAS version 3.0 calculations. Based on the NAIRAS modeled effective dose rate, a 1000-hour commercial flight crew is only exposed to 11.9 mSv over a typical 1000-hour year, much lower than the ARMAS estimate as well as the ICRP recommendation.

Considering the dose rates for absorbed dose in silicon, dose equivalent, and ambient dose equivalent, there is very good agreement between NAIRAS and ARMAS. Overall, for the majority of cruise altitude segments, the mean (and median) dose rates are within the ARMAS uncertainty of 24%. This result provides confidence in using the NAIRAS model for making dose exposure estimates for flight trajectories. Furthermore, comparing dose rate estimates from NAIRAS version 2.0 to NAIRAS version 3.0 shows substantial improvements in the modeled dose rate calculations.

While this dataset provides a fairly representative sample of corporate aircraft flight paths, the majority of flights occurred over northern hemisphere midlatitudes, particularly in the United States. For a more thorough evaluation, a wider range of flights should be considered. Currently, there is an ongoing effort to evaluate the larger collection of flights (over 1000 flights) using the ARMAS FM dosimeter occurring between 2013 and 2023. This dataset consists of flights ranging from 8 km – 550 km in altitude and includes NASA, commercial and corporate flights, as well as high altitude balloons, commercial suborbital, and the International Space Station (ISS). This evaluation is expected to yield a broader understanding of the expected dose rates as well as a more robust comparison with NAIRAS version 3.0.

**Acknowledgements**

The NAIRAS model extension from the atmosphere to space was funded by the NASA Engineering and Safety Center (NESC) assessment TI-19-01468. The improvements in SEP event spectral fitting and cutoff rigidity modeling were funded by the NASA Science Mission Directorate, Heliophysics Division, Space Weather Science Applications Program.

**Data Availability Statement**

The NAIRAS RoR service is available at CCMC (Zheng, 2023). Descriptions of the NAIRAS model are given by Mertens et al. (2010, 2012, and 2013). The ARMAS database can be accessed at https://sol.spacenvironment.net/ARMAS_Archive/ARMAS_dirIP_Report_UUID_YMDhms_L1L4_data_txts/

## References

American Meteorological Society (2007), Integrating space weather observation and forecasts into aviation operations. Technical Report, American Meteorological Society Policy Program & SolarMetrics, Washington, D. C.

Bennett, L. G. I., Lewis, B. J., Bennett, B. H., McCall, M. J., Bean, M., Doré, L., and Getley, I. L.
(2013), A survey of the cosmic radiation exposure of Air Canada pilots during maximum galactic radiation conditions in 2009. *Radiat. Meas., 49,* 103 – 108.

Copeland, K, Sauer, H. H., Duke, F. E., and Friedberg, W. (2008), Cosmic radiation exposure on aircraft occupants on simulated high-latitude flights during solar proton events from 1 January 1986 through 1 January 2008. *Adv. Space Res., 42*, 1008 – 1029.

Copeland, K., Friedberg, W., Sato, T., and Niita, K. (2012), Comparison of fluence-to-dose conversion coefficients for deuterons, tritons, and helions, *Radiation Protection Dosimetry, 148*(3), 344 – 351. https://doi.org/10.1093/rpd/ncr035.

Copeland, K. (2017), CARI-7A: Development and validation. *Radiation Protection Dosimetry,* **178**(4), 419 – 431. https://doi.org/10.1093/rpd/ncw369.

Dyer, C., Hands, A., Lei, F., Truscott, P., Ryden, K. A., Morris, P., Getley, I., Bennett, L., Bennett,
B., and Lewis, B. (2009), Advances in measuring and modeling the atmospheric radiation environment, *IEEE Trans. Nucl. Sci., 56*(8), 3415 – 3422.

Gopalswamy, N., Yashiro, S., Lara, A., Kaiser, M. L., Thompson, B. J., Gallagher, P. T., and Howard, R. A. (2003), Large solar energetic particle events of solar cycle 23: A global view. *Geophys. Res. Lett., 30*(12), 8015. https://doi.org/10.1029/2002GL016435.

ICRP (2007), ICRP Publication 103: The 2007 Recommendations of the International Commission
on Radiological Protection, *37*(2-4), Elsevier, Oxford.

IEC (2006), Process management for avionics—Atmospheric radiation effects—Part 1: Accommodation of atmospheric radiation effects via single event effects within avionics electronic equipment. IEC/TS 62396-1:2006(E), International Electrontechnical Commission.

Lindborg, L., and Nikjoo, H. (2011), Microdosimetry and radiation quality determinations in radiation protection and radiation therapy. *Radiat. Prot. Dosim., 143*(2-4), 402 – 408.

Matthiä, D., Berger, T., Mrigakshi, A. I., and Reitz, G. (2013), A ready-to-use galactic cosmic ray model. *Advances in Space Research, 51*(3), 329-338.

https://doi.org/10.1016/j.asr.2012.09.022.

Matthiä, D., Meier, M. M., and Reitz, G. (2014), Numerical calculation of the radiation exposure from galactic cosmic rays at aviation altitudes with the PANDOCA core model. *Space Weather, 12,* 161-171. https://doi.org/10.1002/2013SW001022.

Meier, M. M., Trompier, F., Ambrozova, I., Kubancak, J., Matthiä, D., Ploc, O., et al. (2016), CONCORD: Comparison of cosmic radiation detectors in the radiation field at aviation altitudes, *Journal of Space Weather and Space Climate, 6.* https://doi.org/10.1051/swsc/2016017.

Meier, M. M., Copeland, K., Matthiä, D., Mertens, C. J., and Schennetten, K. (2018), First steps toward the verification of models for the assessment of the radiation exposure at aviation altitudes during quiet space weather conditions. *Space Weather, 16,* 1269-1276, https://doi.org/10.1029/2018SW001984.

Mertens, C. J., Kress, B. T., Wiltberger, M., Blattnig, S. R., Slaba, T. S., Solomon, S. C., and Engel, M. (2010), Geomagnetic influence on aircraft radiation exposure during a solar energetic particle event in October 2003. *Space Weather, 8,* S03006, https://doi.org/10.1029/2009SW000487.

Mertens, C. J., Kress, B. T., Wiltberger, M., Tobiska, W. K., Grajewski, B., and Xu, X. (2012), Atmospheric ionizing radiation from galactic and solar cosmic rays, in *Current Topics in Ionizing Radiation Research*, edited by M. Nenoi, InTech Publisher, (ISBN 978-953-51-0196-3).

Mertens, C. J., Meier, M. M., Brown, S., Norman, R. B., and Xu, X. (2013). NAIRAS aircraft radiation model development, dose climatology, and initial validation. *Space Weather, 11*(10), 603-635, https://doi.org/10.1002/swe.20100.

Mertens, C. J., Gronoff, G. P., Phoenix, D., Zheng, Y., Petrenko, M., Buhler, J., Jun, I., Minow, J., and Willis, E. (2023a), NAIRAS Ionizing Radiation Model: Extension from Atmosphere to Space. Technical Publication, NASA Langley Research Center, Hampton, VA.

Mertens, C. J., Gronoff, G. P., Zheng, Y., Petrenko, M., Buhler, J., Phoenix, D., Willis, E., Jun, I., Minow, J. (2023b), NAIRAS Model Run-On-Request Service at CCMC. *Space Weather, 21*(5), https://doi.org/10.1029/2023SW003473.

Mertens, C. J., Gronoff, G. P., Zheng, Y., Buhler, J., Willis, E., Petrenko, M., Phoenix, D., Jun, I., and Minow, J. (2023c), NAIRAS Atmospheric and Space Radiation Environment Model. *IEEE Transactions on Nuclear Science,* https://doi.org/10.1109/TNS.2023.3330675.

Tobiska, W. K., et al. (2016), Global real-time dose measurements using the Automated

566 Radiation Measurements for Aerospace Safety (ARMAS) system. *Space Weather, 14,*
567 1053–1080, https://doi.org/10.1002/2016SW001419.
568
569 Tysganenko, N. A. (1989), Determination of magnetic current system parameters and
570 development of experimental geomagnetic field models based on data from IMP and
571 HEOS satellite. *Planetary and Space Science, 37,* 5 – 20.
572
573 Tysganenko, N. A. and Sitnov, N. I. (2005), Modeling the dynamics of the inner magnetosphere
574 during strong geomagnetic storms. *J. Geosphys. Res.,* 110, A03208,
575 https://doi.org/10.1029/2004JA010798.
576
577 Zheng, Y. (2023). User interface to NAIRAS model (Version 3.0) run-on-request service.
578 [Software]. https://ccmc.gsfc.nasa.gov/models/NAIRAS~3.0